

Article

Efficient Diesel Desulfurization by Novel Amphiphilic Polyoxometalate-Based Hybrid Catalyst at Room Temperature

Jie Zhao ¹, Bingquan Wang ², Rui Wang ^{1,*} , Ivan V. Kozhevnikov ³  and Korchak Vladimir ⁴¹ School of Environmental Science and Engineering, Shandong University, Qingdao 266237, China² School of Chemistry and Molecular Engineering, Qingdao University of Science and Technology, Qingdao 266042, China³ Department of Chemistry, University of Liverpool, Liverpool L69 7ZD, UK⁴ N. N. Semenov Federal Research Center of Chemical Physics, Russian Academy of Sciences, Moscow 119991, Russia

* Correspondence: wangrui@sdu.edu.cn

Abstract: Amphiphilic hybrid catalysts were prepared by modifying $[\text{SMo}_{12}\text{O}_{40}]^{2-}$ with tetrabutylammonium bromide (TBAB), 1-butyl-3-methylimidazole bromide (BMIMBr) and octadecyl trimethyl ammonium bromide (ODAB), respectively. The prepared catalysts were characterized by IR, XRD, SEM, TG and XPS. The desulfurization performance of the catalysts was investigated in model oil and actual diesel using hydrogen peroxide (H_2O_2) as an oxidant and acetonitrile as an extractant. All catalysts exhibited favorable activity for removing sulfur compounds at room temperature. Dibenzothiophene (DBT) can be nearly completely removed using $\text{SMo}_{12}\text{O}_{40}^{2-}$ -organic catalysts within a short reaction time. For different sulfur compounds, the $[\text{TBA}]_2\text{SMo}_{12}\text{O}_{40}$ catalyst showed a better removal effect than the $[\text{BMIM}]_2\text{SMo}_{12}\text{O}_{40}$ and $[\text{ODA}]_2\text{SMo}_{12}\text{O}_{40}$ catalyst. The $[\text{TBA}]_2\text{SMo}_{12}\text{O}_{40}$ dissolved in extraction solvent could be reused up to five times in an oxidative desulfurization (ODS) cycle with no significant loss of activity. The $[\text{BMIM}]_2\text{SMo}_{12}\text{O}_{40}$ performed as a heterogeneous catalyst able to be recycled from the ODS system and maintained excellent catalytic activity. The catalysts showed a positive desulfurization effect in real diesel treatment. Finally, we described the ODS desulfurization mechanism of DBT using $\text{SMo}_{12}\text{O}_{40}^{2-}$ -organic hybrid catalysts. The amphiphilic hybrid catalyst cation captures DBT, while $\text{SMo}_{12}\text{O}_{40}^{2-}$ reacts with the oxidant H_2O_2 to produce peroxy-active species. DBT can be oxidized to its sulfone by the action of peroxy-active species to achieve ODS desulfurization.

Keywords: desulfurization; diesel; polyoxometalate; oxidation catalysis

Citation: Zhao, J.; Wang, B.; Wang, R.; Kozhevnikov, I.V.; Vladimir, K. Efficient Diesel Desulfurization by Novel Amphiphilic Polyoxometalate-Based Hybrid Catalyst at Room Temperature. *Molecules* **2023**, *28*, 2539. <https://doi.org/10.3390/molecules28062539>

Academic Editors: Maria Luisa Di Gioia, Luísa Margarida Martins and Isidro M. Pastor

Received: 9 February 2023

Revised: 7 March 2023

Accepted: 9 March 2023

Published: 10 March 2023



Copyright: © 2023 by the authors. Licensee MDPI, Basel, Switzerland. This article is an open access article distributed under the terms and conditions of the Creative Commons Attribution (CC BY) license (<https://creativecommons.org/licenses/by/4.0/>).

1. Introduction

Diesel is an important energy source and plays a vital role in industrial production [1,2]. Sulfur-containing compounds are one of the main pollutants in diesel, and its existence will bring many adverse effects. The combustion of sulfur-containing compounds produces SO_x , which can cause air pollution and acid rain [3–5]. In addition, the presence of sulfur compounds in diesel can also poison the catalytic converter and corrode internal refinery components. As a result, countries around the world have implemented and proposed more stringent fuel standards [6]. Most countries require that the sulfur content in fuel cannot be higher than 10 ppm [7–10]. At present, fuel desulfurization technology is mainly divided into two categories: hydrodesulfurization (HDS) and non-hydrodesulfurization. HDS is the most widely used desulfurization technology in the industry [11,12]. HDS requires hydrogen consumption and high temperature and pressure operating conditions, which increase equipment input and economic costs [13,14]. The conventional catalytic HDS process has the least efficiency for the catalytic hydrodesulfurization of thiophene sulfides [15]. Therefore, the high input cost and poor removal effect of thiophene sulfides limit the development and application of HDS technology. Non-hydrodesulfurization

technologies include extractive desulfurization (EDS), biological desulfurization (BDS), adsorption desulfurization (ADS), and oxidative desulfurization (ODS) technologies [16]. Among them, ODS is considered to be the industrial replacement technique for HDS with the most potential because of its mild reaction conditions, good removal effect with regard to thiophene sulfides, and low input costs [17]. ODS refers to the method in which sulfides are oxidized into corresponding sulfoxides/sulfones under the action of oxidants and catalysts and are removed from the oil by extraction, adsorption or distillation [18–21].

The choice of oxidant and catalyst has an important influence on ODS performance. Oxygen (O_2), ozone (O_3), hydrogen peroxide (H_2O_2), and organic peroxides are normally used to act as oxidants in ODS systems [3,17]. Among them, H_2O_2 is widely used in the ODS process due to its strong oxidizing ability and environmental friendliness [22–25]. Because of their unique molecular structure and excellent chemical properties, polyoxometalates (POMs) have always been hot materials in the field of catalysis [26–28]. Researchers have found that changing the heteroatom in Keggin heteropoly anions leads to different redox properties. Himeno et al. performed a systematic analysis of the voltammetric properties of Keggin-type polyoxometalate complexes (α - $[XMo_{12}O_{40}]^{n-}$ ($X = S, P, As, Si, Ge$; $n = 2-4$) and α - $[XW_{12}O_{40}]^{n-}$ ($X = S, P, As, Si, Ge, B, Al$; $n = 2-5$) based on alkalinity. The results show that the basicity of the Keggin anions is in the order of $[SMo_{12}O_{40}]^{2-} \approx [XW_{12}O_{40}]^{3-}$ ($X = P, As$) \ll $[XMo_{12}O_{40}]^{3-}$ ($X = P, As$) $<$ $[XW_{12}O_{40}]^{4-}$ ($X = Si, Ge$) \ll $[XMo_{12}O_{40}]^{4-}$ ($X = Si, Ge$) $<$ $[XW_{12}O_{40}]^{5-}$ ($X = B, Al$) [29]. Wedd's group demonstrated that the sulfo-polyoxometalate anion clusters $[S_2W_{18}O_{62}]^{4-}$, $[S_2Mo_{18}O_{62}]^{4-}$ and $[SMo_{12}O_{40}]^{2-}$ can be activated photochemically to oxidize the organic substrates benzyl alcohol, ethanol, and (–)-menthol [30]. They then subsequently found in reduction studies of Mo and W polyoxometalate anions in both ionic liquid and conventional solvent (electrolyte) media that Mo polyoxometalates are always easier to reduce than their W counterparts, and that reduced W polyoxometalates are more stable than their isostructural Mo analogues (these differences are possibly associated with the higher electron affinity of Mo(VI) sites and the higher proton affinity of -O- sites in Mo polyoxometalates, which makes the Mo moieties easier to reduce and also more prone to attack by protons than their W counterparts) [31]. However, when POMs are employed as ODS catalysts, the fact that POMs are insoluble in the organic oil phase hinders the effective contact between the catalyst and sulfur compounds, affecting the ODS efficiency [32,33]. In order to solve this problem, some scholars proposed the addition of an extractant into the ODS system [34,35]. The lipophilicity oil phase and hydrophilic extraction phase form a two-phase system in which the POM is dissolved in the extraction phase. Sulfur compounds in the oil phase are extracted into the aqueous phase, and react with oxidants under catalytic action to form corresponding polar sulfones. Although the problem of insolubility of the POM catalyst can be solved by adding extractant into the ODS system, the mass transfer resistance between the oil phase and the extraction phase still hinders the desulfurization efficiency and reaction rate.

For this reason, many researchers have proposed to introduce amphiphilic component into the POM to reduce the mass transfer resistance between the two phases. The amphiphilic POM-based catalyst can make use of the lipophilicity of the cation to make the sulfides in the oil and the oxidation active center have better contact so that the desulfurization reaction can proceed faster and better [36,37]. POMs can be modified by organic units such as quaternary ammonium salts, ionic liquids, oligomers, etc. [38]. To date, a lot of work on amphiphilic POM-based catalysts has been reported. Li et al. synthesized the amphiphilic catalyst by the combination of quaternary ammonium salt and phosphotungstate, and studied the effect of different quaternary ammonium cations on the performance of the catalyst [39]. The results showed that $[(C_{18}H_{37})_2N(CH_3)_2]_3[PW_{12}O_{40}]$ had excellent activity. When the temperature was 30 °C, the desulfurization rate could reach 100% after 80 min of reaction. In 2006, Lv et al. reported another amphiphilic catalyst $[(C_{18}H_{37})_2N(CH_3)_3]_4[H_2NaPW_{10}O_{36}]$ [40], which can complete the highly active catalytic oxidation reaction in an ODS system with high sulfur content. Wang's group prepared

three hybrid POM materials [HPMo][TMAC]₂, [HPMo][DTAC]₂, and [HPMo][HTAC]₂ by using modified phosphomolybdic acid (HPMo) with tetramethylammonium chloride (TMAC), dodecyltrimethylammonium chloride (DTAC), and cetyltrimethylammonium chloride (HTAC). Under the condition of H₂O₂ as the oxidant, the catalytic activity was compared in the ODS system. When [HPMo][HTAC]₂ was used as a catalyst, the conversion rate of dibenzothiophene (DBT) reached 96% at 60 °C for 180 min. The reason that [HPMo][HTAC]₂ has better catalytic performance is that the longer hexadecyl chain in the structure is not only more beneficial to the wrapping of DBT, but is also beneficial to the formation of a stable emulsion system containing a high DBT concentration [41]. Susana et al. reported three organic-inorganic hybrid catalysts-based [PW₁₁Zn(H₂O)O₃₉]⁵⁻ [42]. As a phase transfer agent, the quaternary ammonium cation can promote the effective mass transfer between the oil phase and the extraction phase, and improve the desulfurization rate. Under the action of the catalyst processing tetrabutylammonium bromide cation, the reaction has a favorable removal effect on different sulfur compounds. Li et al. studied amphiphilic catalysts with a core-shell structure [15]. The hydrophilic core is composed of phosphotungstic acid (PWO) clusters as the catalytic center, and the lipophilic shell consisted of long chain alkyl-imidazole or pyridine cations. DBT could be completely oxidized at 40 °C within 40 min under the catalysis of [C₁₆MIM]₃PWO. This method is useful for actual diesel desulfurization. Amphiphilic ODS catalysts are frequently reported [37,43]. The design of an amphiphilic ODS catalyst with high activity, selectivity, and recyclability is a research hotspot in the field of fuel desulfurization.

In this paper, we studied three kinds of amphiphilic hybrid catalysts based on [SMo₁₂O₄₀]²⁻. The polyacid anion [SMo₁₂O₄₀]²⁻ is a saturated α -Keggin type POM. In the POM, all of the Mo exhibit the geometric environment of the {MoO₆} octahedron. The central S atom is surrounded by eight oxygen atoms connected to it, forming a small cube at the center of the entire polyacid. The whole α -Keggin POM is composed of 12 {MoO₆} octahedrons connected by common edges and common angles, and then connected with the center {SO₄} unit at common angles. The S element in [SMo₁₂O₄₀]²⁻ anion appears as the sulfate species. POM with the S⁶⁺ heteroatom is rare. The S⁶⁺ heteroatom helps to disperse the negative charges on the surface of the POM and makes the POM more stable. Different hybrid catalysts were prepared by modifying [SMo₁₂O₄₀]²⁻ with a tetrabutylammonium (TBA), 1-butyl-3-methylimidazolium (BMIM), and octadecyldimethylammonium (ODA) cation. The catalytic performance of catalysts was evaluated in model oil and actual diesel using H₂O₂ as the oxidant and acetonitrile as the extractant. Various reaction conditions that affect desulfurization efficiency are optimized in the ODS process and the recovery performance of catalysts was investigated. To the best of our knowledge, this is the first report on the application and optimization of the [SMo₁₂O₄₀]²⁻-organic hybrid catalysts in the ODS system.

2. Results and Discussion

2.1. Characterization of Catalysts

The hybrid catalysts based on [SMo₁₂O₄₀]²⁻ were characterized by IR. The characteristic absorption peaks of [SMo₁₂O₄₀]²⁻ with a Keggin structure are shown in Figure 1. Due to the difference of organic cations, the characteristic peak of the polyanion has shifted to different degrees. The characteristic bands of S-O in catalyst structures occurs at 1151, 1163 and 1111 cm⁻¹, respectively. The peaks of wave number at 952, 957 and 950 cm⁻¹ are attributed to Mo=O. The (Mo-O-Mo) symmetric or asymmetric vibration approximately appears in 885–880 cm⁻¹ and 778–765 cm⁻¹ [44]. These characteristic peaks indicate the presence of [SMo₁₂O₄₀]²⁻-polyoxometalate. In the [TBA]₂SMo₁₂O₄₀ catalyst, the peaks at 2962, 2874 and 1481 cm⁻¹ belong to the vibration of the TBA cation [45,46]. In the [BMIM]₂SMo₁₂O₄₀ catalyst, the peaks observed at 3144 and 3108 cm⁻¹ are attributed to the imidazole ring's hydrogen. The stretching absorption peak of n-butyl's hydrogenate can be assigned as 2957 and 2926 cm⁻¹. The characteristic peaks of the imidazole ring are observed at 1566 and 1465 cm⁻¹ [43,47]. In the [ODA]₂SMo₁₂O₄₀ catalyst, the vibration peaks at 2918, 2851 and 1469 cm⁻¹ are characteristic of an ODA cation structure [27]. Figure 2

shows the IR spectra of the $[\text{BMIM}]_2\text{SMo}_{12}\text{O}_{40}$ catalyst before and after recovery. The IR of the recovered $[\text{BMIM}]_2\text{SMo}_{12}\text{O}_{40}$ catalyst showed that no obvious characteristic peak was destroyed, indicating that the structure of the recovered catalyst remained intact.

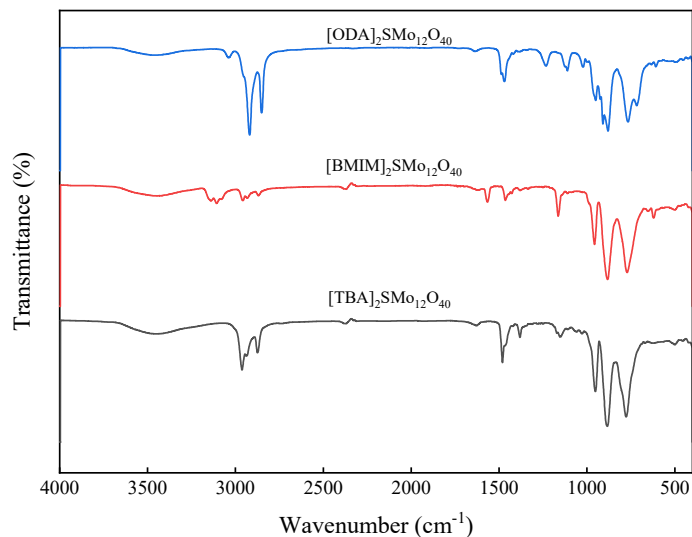


Figure 1. IR spectra of the catalysts.

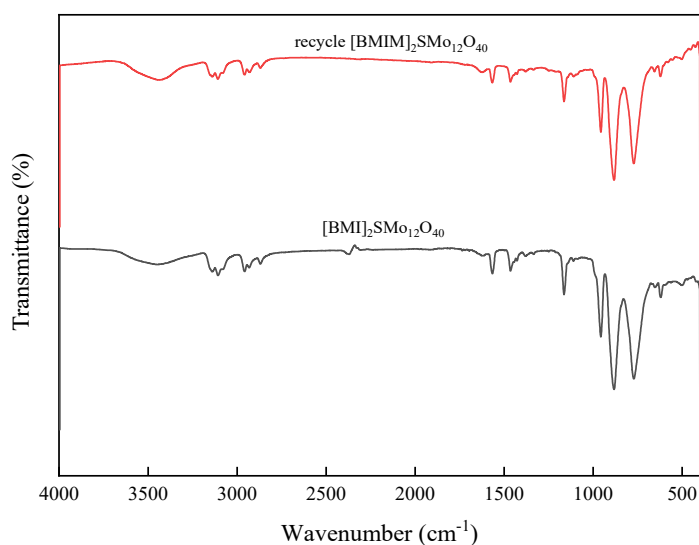


Figure 2. IR spectra of the $[\text{BMIM}]_2\text{SMo}_{12}\text{O}_{40}$ catalyst before and after recovery.

The XRD patterns of catalysts are shown in Figure 3. The strong characteristic peak appeared in the 2θ range of 6.5° – 10° , indicating the ordering of the Keggin bulk structure of the polyoxoanion [48]. Due to the introduction of different organic cations, some weak characteristic peaks appeared in different 2θ range. The intensity of characteristic peaks in $[\text{TBA}]_2\text{SMo}_{12}\text{O}_{40}$ are weaker than $[\text{BMIM}]_2\text{SMo}_{12}\text{O}_{40}$ and $[\text{OTA}]_2\text{SMo}_{12}\text{O}_{40}$, indicating that the $[\text{SMo}_{12}\text{O}_{40}]^{2-}$ group is finely dispersed with the mixing of TBAB [41].

SEM images of the prepared catalysts at different magnifications are shown in Figure 4. It can be seen from the SEM image that $[\text{SMo}_{12}\text{O}_{40}]^{2-}$ performs as a small spherical particle with an irregular surface. The TBA cation component is in the shape of a short rod and is connected with the polyacid anion. The overall structure of the amphiphilic $[\text{TBA}]_2\text{SMo}_{12}\text{O}_{40}$ catalyst is relatively loose. $[\text{BMIM}]_2\text{SMo}_{12}\text{O}_{40}$ is composed of larger particles and has long rod-shaped ionic liquid components. The overall structure of $[\text{ODA}]_2\text{SMo}_{12}\text{O}_{40}$ is relatively compact, and its surface is covered with a waxy layer

because of the long-chain alkyl substitutes. $[\text{ODA}]_2\text{SMo}_{12}\text{O}_{40}$ is a lamellar structure, and the active center $[\text{SMo}_{12}\text{O}_{40}]^{2-}$ is attached to its surface.

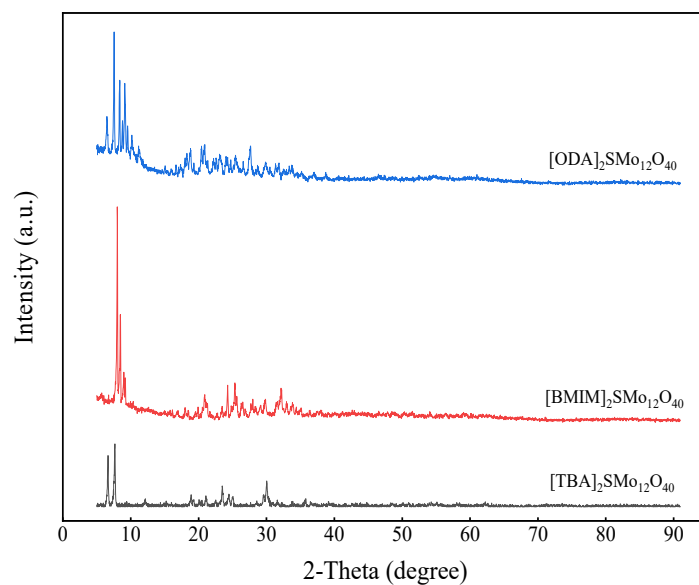


Figure 3. XRD patterns of the catalysts.

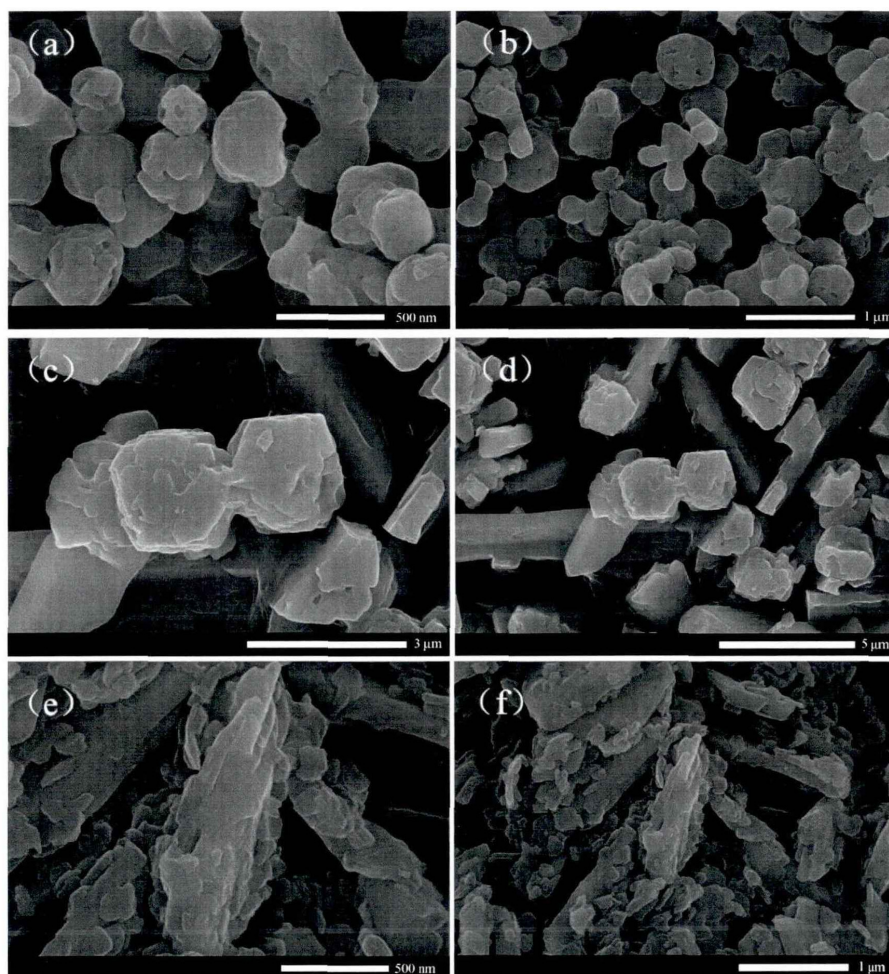


Figure 4. SEM images of (a,b) $[\text{TBA}]_2\text{SMo}_{12}\text{O}_{40}$, (c,d) $[\text{BMIM}]_2\text{SMo}_{12}\text{O}_{40}$, and (e,f) $[\text{ODA}]_2\text{SMo}_{12}\text{O}_{40}$ catalysts.

The thermal stability of hybrid catalysts was studied by thermogravimetric analysis. The obtained results are shown in Figure 5. $[\text{TBA}]_2\text{SMo}_{12}\text{O}_{40}$ and $[\text{BMIM}]_2\text{SMo}_{12}\text{O}_{40}$ have weight loss regions between 240–600 °C and 220–600 °C, respectively. This demonstrates that $[\text{TBA}]_2\text{SMo}_{12}\text{O}_{40}$ and $[\text{BMIM}]_2\text{SMo}_{12}\text{O}_{40}$ begin to decompose. The $[\text{OTA}]_2\text{SMo}_{12}\text{O}_{40}$ catalyst showed two weight loss areas. The first small weight loss of 2.5% observed between 36 and 78 °C is attributed to the removal of physically adsorbed water. The weight loss region (~50.7%) between 220–600 °C is assigned to the $[\text{OTA}]_2\text{SMo}_{12}\text{O}_{40}$ that is beginning to decompose. The results of thermogravimetric analysis show that the decomposition temperature of the catalysts was higher than the reaction temperature of this experiment.

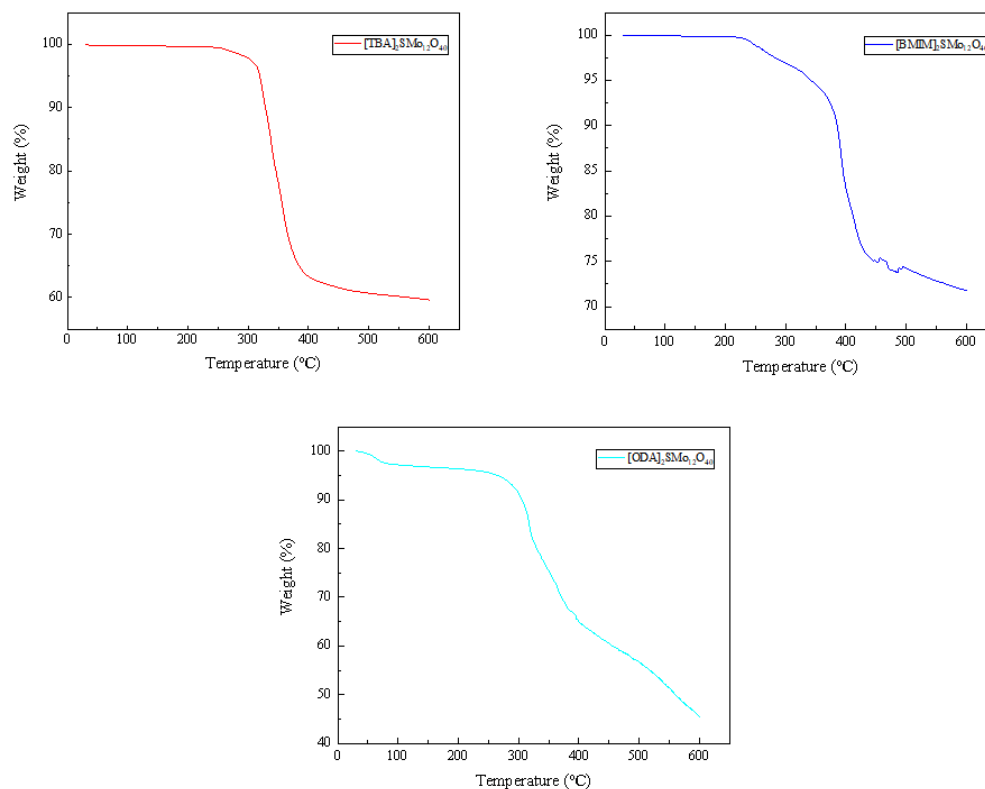


Figure 5. Thermogravimetric analysis of the catalysts.

In order to determine the state of elements in the catalyst, an XPS characterization was performed. The results obtained are shown in Figure 6. Through the spectroscopy of Mo element in the $[\text{TBA}]_2\text{SMo}_{12}\text{O}_{40}$ catalyst, it can be found that the binding energy of Mo $3d_{5/2}$ appears at 232.7 eV, indicating that the small peak is attributed to Mo^{6+} [49]. In the S 2P spectra of the $[\text{TBA}]_2\text{SMo}_{12}\text{O}_{40}$ catalyst, absorption peaks of S $2p_{3/2}$ and S $2p_{1/2}$ were observed at 169.18 and 170.36 eV, and are attributed to the sulfate species contribution [50,51]. The $[\text{SMo}_{12}\text{O}_{40}]^{2-}$ with S^{6+} heteroatom has an oxidizing ability.

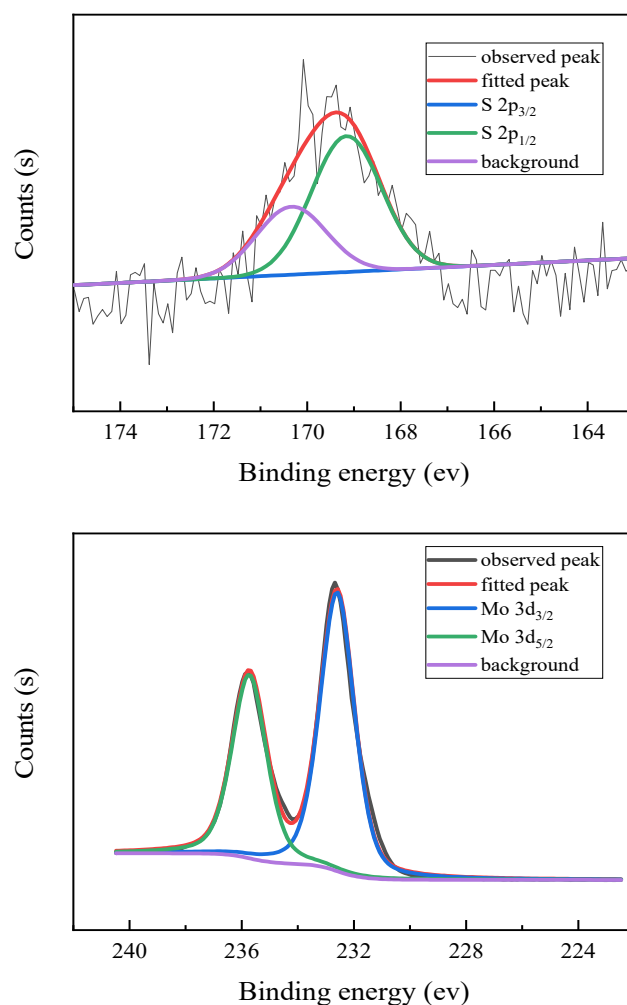


Figure 6. XPS spectra of $[\text{TBA}]_2\text{SMo}_{12}\text{O}_{40}$ catalyst.

2.2. Optimization of ODS System

The optimization in the ODS system was performed with the $[\text{TBA}]_2\text{SMo}_{12}\text{O}_{40}$ catalyst. Various factors affecting desulfurization efficiency were investigated, including catalyst dosage, oxygen/sulfur molar ratio, and reaction temperature.

The effect of different catalyst dosages (catalyst dosage to the mass ratio of model oil) on the ODS efficiency were shown in Figure 7. The experimental conditions were set to an initial sulfur content of 500 ppm, an O/S molar ratio of 10, and a temperature of 60 °C. As shown in Figure 8, when no catalyst is added, the DBT removal rate is only 58.62%, depending on the extraction of acetonitrile and the oxidation capacity of H_2O_2 . In the presence of the catalyst, the desulfurization rate exceeded 91% when the reaction only proceeded for 3 min. In the initial stage of the reaction, the increase in the catalyst dosage is beneficial in improving the reaction rate. When the amount of catalyst increased from 0.21 g to 0.63 g, the desulfurization rate gradually increased. When the catalyst dosage was 0.84 g, the desulfurization rate decreased compared with that of 0.63 g. The desulfurization reaction basically reached a stable desulfurization effect in 10 min. When the catalyst dosage was 0.63 g, the best desulfurization rate (96.1%) could be obtained within 10 min. Therefore, the optimal catalyst dosage was determined to be 0.63 g (the catalyst dosage accounted for 1.5 wt% of the model oil quality).

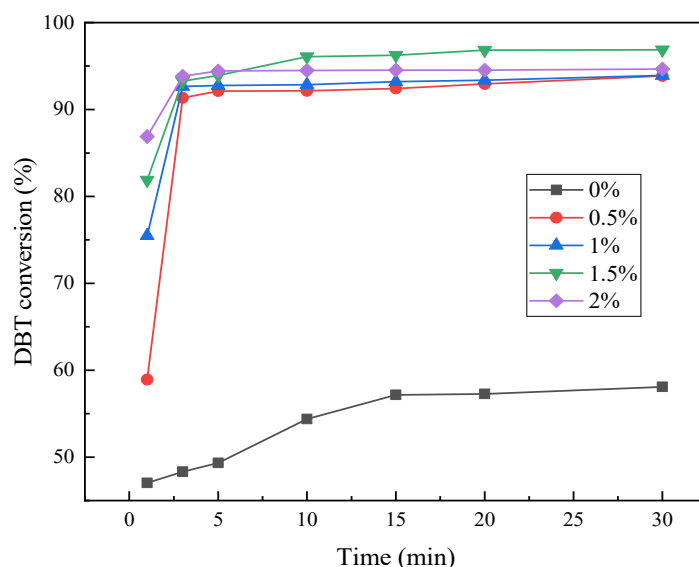


Figure 7. Influence of catalyst dosage on the conversion of DBT.

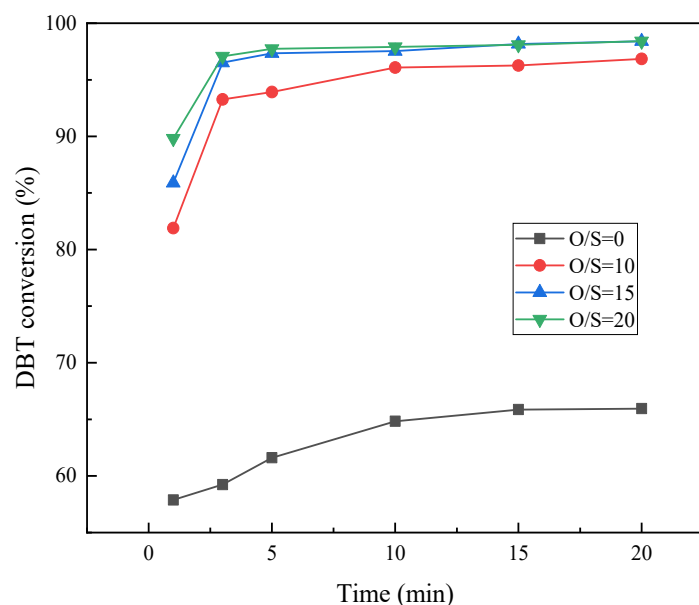


Figure 8. Influence of O/S molar ratio on the conversion of DBT.

The O/S molar ratio plays an important role in the desulfurization effect. Reactive oxygen molecules come from H_2O_2 . According to the chemical equation of the DBT oxidation reaction, 1 mol DBT can be oxidized to the corresponding sulfone by 2 mol H_2O_2 . However, due to the side reaction of self-decomposition of H_2O_2 in the reaction process, a larger amount of oxidant is often needed in the experiment. The influence of the O/S molar ratio was studied at 60 °C, using the model oil with an initial sulfur content of 500 ppm and a catalyst dosage of 0.63 g. The DBT conversion rates at different O/S molar ratios are shown in Figure 8. In the absence of oxidant, a desulfurization rate of 65.94% could be obtained within 20 min. With the addition of the oxidant, the desulfurization rate increased rapidly in a short time. The O/S molar ratio is directly proportional to the desulfurization rate and the reaction rate. When the O/S molar ratio was 20, the maximum desulfurization rate reached 98.40%, which was basically consistent with the desulfurization effect when the O/S molar ratio was 15 (desulfurization rate: 98.39%). Considering economic costs and energy utilization, the optimal O/S molar ratio was set to 15 for the following experiments.

Figure 9 shows the conversion rate of DBT at different temperatures, maintaining the other experimental conditions (the model oil with an initial sulfur content of 500 ppm, a catalyst dosage of 0.63 g and an O/S molar ratio of 15). The temperature increase is beneficial to increasing the reaction rate within 5 min. The DBT oxidation reaction at different temperatures reached equilibrium in 10 min. It is worth noting that a lower temperature can often achieve a higher desulfurization efficiency. The reason is that the rising temperature accelerates the decomposition of H_2O_2 , which is not conducive to the continued progress of the DBT oxidation reaction, leading to less sulfur removal. Under the condition that the initial sulfur content is 500 ppm, O/S = 15, and the dosage of catalyst accounts for 1.5 wt% of the model oil quality, the DBT conversion rate reached 99.89% within 10 min at room temperature, achieving an ultra-fast and efficient desulfurization process. Desulfurization at room temperature can greatly reduce the economic cost and ensure fuel quality. Hence, the optimal reaction temperature is room temperature.

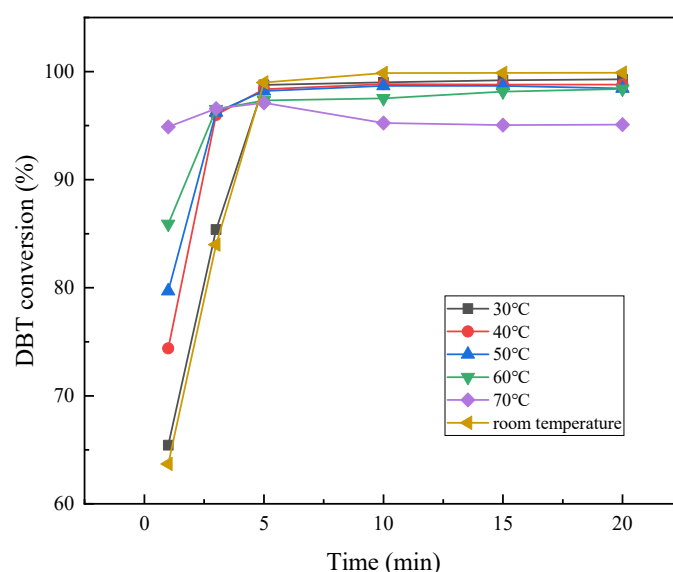


Figure 9. Influence of temperature on conversion of DBT.

2.3. Comparison of Desulfurization Performance of Three Hybrid Catalysts Based $[SMo_{12}O_{40}]^{2-}$

Under the above optimized reaction conditions, the desulfurization performance of the $[TBA]_2SMo_{12}O_{40}$ catalyst for different sulfur compounds (DBT, BT and 4,6-DMDBT) was investigated (Figure 10). For the removal of DBT, a high conversion rate of 99.89% was achieved when the reaction was carried out for 10 min. BT and 4,6-DMDBT are sulfur compounds that are more difficult to oxidize than DBT. Under the catalysis of $[TBA]_2SMo_{12}O_{40}$, the removal rates of BT and 4,6-DMDBT reached 97.06% and 95.20%, respectively, when the reactions were carried out for 90 min. In a comparison of the ODS activity of different catalysts in a previous work and in this study (Table 1), the $[TBA]_2SMo_{12}O_{40}$ catalyst was shown to have a generally excellent desulfurization performance for different sulfides. The desulfurization performance of $[BMIM]_2SMo_{12}O_{40}$ and $[ODA]_2SMo_{12}O_{40}$ was also investigated by using the previous optimized reaction conditions (Figure 10). When $[BMI]_2SMo_{12}O_{40}$ is used as a catalyst, the DBT removal rate can reach 99.81% within 15 min at room temperature. After the reactions proceeded for 90 min, BT and 4,6-DMDBT reached 93.05% and 89.21% conversion, respectively. Using an $[ODA]_2SMo_{12}O_{40}$ catalyst, a 99.47% DBT removal rate was reached at 60 min. The conversion rates for BT and 4,6-DMDBT can be reached at 85.24% and 89.35% levels within 2 h, respectively.

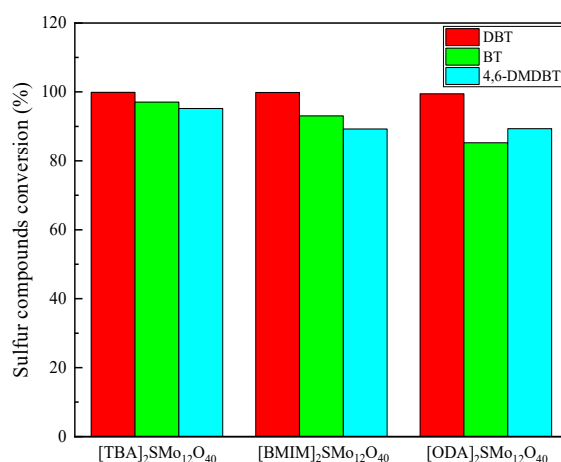


Figure 10. Desulfurization performance of catalysts for different sulfur compounds.

Table 1. Desulfurization performance of catalysts in a previous work and in this study.

Catalyst	Sulfur Compounds	Conversion (%)	Reaction Conditions	Reference
PMo ₁₂ @UiO-67	DBT	99.50%	O/S = 3.1, 50 °C	[52]
PW12@UiO-67	DBT	99.50%	70 °C	[53]
[Bmim] ₃ PMo ₁₂ O ₄₀	DBT	100%	O/S = 3, 60 °C	[54]
[(C ₈ H ₁₇) ₃ NCH ₃] ₃ PMo ₁₂ O ₄₀ /γ-Fe ₂ O ₃ @SiO ₂ @mSiO ₂	DBT	100%	120 °C	[55]
[C ₈ quin] ₄ Mo ₈ O ₂₆	DBT	99.2%	60 °C	[56]
[TBA] ₂ SMO ₁₂ O ₄₀	DBT	99.89%	O/S = 15, 60 °C	This work
[TBA] ₂ SMO ₁₂ O ₄₀	BT	97.06%	O/S = 15, 60 °C	This work
[TBA] ₂ SMO ₁₂ O ₄₀	4,6-DMDBT	95.20%	O/S = 15, 60 °C	This work

The desulfurization effect of three organic-inorganic hybrid catalysts for different sulfides follows the following sequence: [TBA]₂SMO₁₂O₄₀ > [BMIM]₂SMO₁₂O₄₀ > [ODA]₂SMO₁₂O₄₀. The [TBA]₂SMO₁₂O₄₀ catalyst showed the best desulfurization efficiency. The catalytic activity of POMs-based hybrid catalysts is affected by the linked organic cations. Li et al. prepared a series of surfactant-type decatungstates catalysts [23]. They pointed out that the increase of the carbon chain length of the quaternary ammonium cation was beneficial to the enhancement of the activity of the catalyst. Zhuang et al. synthesized three molybdovanadophosphoric POM-based catalysts by contacting H₅PMo₁₀V₂O₄₀ with different ionic liquids [57]. They also reached a conclusion: The removal efficiency of the sulfur compound improved with the increase of the alkyl chain length of the catalyst. However, Lu et al. mentioned that quaternary ammonium cations with too long carbon chains may cause steric effects, reducing catalytic activity [49]. In our work, we observed differences in the solubility of three hybrid catalysts containing different cations in the acetonitrile. [TBA]₂SMO₁₂O₄₀ is fully soluble in acetonitrile, allowing more effective contact between sulfur-containing compounds and oxidizing active substances, thereby obtaining a high desulfurization efficiency. [BMI]₂SMO₁₂O₄₀ and [ODA]₂SMO₁₂O₄₀ are insoluble in the oil phase, as is acetonitrile. Under the condition of magnetic stirring, [BMI]₂SMO₁₂O₄₀ was evenly dispersed in the acetonitrile, while [ODA]₂SMO₁₂O₄₀ showed an agglomeration phenomenon. The poor solubility of [ODA]₂SMO₁₂O₄₀ is the main reason for its low desulfurization efficiency.

Under the catalysis of [TBA]₂SMO₁₂O₄₀ and [BMIM]₂SMO₁₂O₄₀, the activities of the three sulfur compounds all followed this sequence: DBT > BT > 4,6-DMDBT, which is consistent with the report by Li et al. [58]. However, 4,6-DMDBT showed a higher oxidation activity than BT when [ODA]₂SMO₁₂O₄₀ acted as a catalyst. The activity of sulfur compounds is mainly related to electron density around the sulfur atom and steric hindrance.

According to Otsuki's report [59], the electron densities of sulfur atoms in DBT, BT and 4,6-DMDBT are 5.758, 5.739 and 5.760, respectively. The higher the electron density of sulfur atoms in sulfur compounds, the easier it is apt to be oxidized, so DBT is easier to remove than BT. However, the structure of 4,6-DMDBT contains two methyl groups. The effect of steric hindrance makes the removal process of 4,6-DMDBT more difficult. The $[\text{ODA}]_2\text{SMo}_{12}\text{O}_{40}$ catalyst with the long alkyl chain has greater ease in wrapping up the larger molecule of 4,6-DMDBT close to the active center [41]. Hence, 4,6-DMDBT had a better removal effect than BT when using the $[\text{ODA}]_2\text{SMo}_{12}\text{O}_{40}$ catalyst.

2.4. Catalyst Recovery

As excellent ODS catalysts, the recovery performance of $[\text{TBA}]_2\text{SMo}_{12}\text{O}_{40}$ and $[\text{BMI}]_2\text{SMo}_{12}\text{O}_4$ was investigated.

After the desulfurization reaction, $[\text{TBA}]_2\text{SMo}_{12}\text{O}_{40}$ was completely dissolved in the acetonitrile phase and could not be separated from the ODS system as a solid. However, the acetonitrile extraction solution containing the dissolved catalyst could be reused for the removal of sulfur compounds. After each reaction, the upper low-sulfur oil was removed, and the fresh model oil with an initial sulfur content of 500 ppm and H_2O_2 (O/S = 15) were added to start a new round of ODS. The reaction time was set to 10 min. After five consecutive cycles of this, there was no apparent loss of catalyst activity. Figure 11 shows the desulfurization effect of the recovered $[\text{TBA}]_2\text{SMo}_{12}\text{O}_{40}$ catalyst (99.89%, 99.89%, 99.89%, 99.32% and 99.01% of DBT conversion rate after 10 min for the first, to the fifth ODS cycle, respectively). The result showed that the $[\text{TBA}]_2\text{SMo}_{12}\text{O}_{40}$ catalyst dissolved in acetonitrile still had an excellent catalytic activity after repeated use.

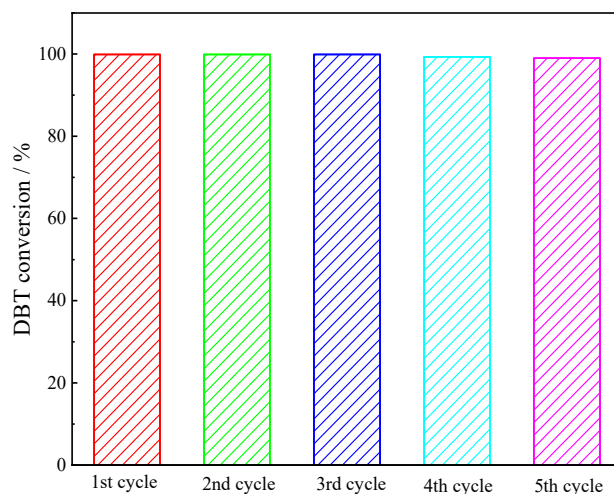


Figure 11. Desulfurization performance of reused $[\text{TBA}]_2\text{SMo}_{12}\text{O}_{40}$ catalyst.

$[\text{BMIM}]_2\text{SMo}_{12}\text{O}_{40}$ performs heterogeneous catalysis in an ODS system. At the end of the reaction, the catalyst deposited on the bottom of the container was filtered, washed with distilled water, and dried in an oven. The desulfurization performance of the recovered $[\text{BMI}]_2\text{SMo}_{12}\text{O}_{40}$ catalyst was evaluated in the optimized desulfurization system. After 15 min of reaction, the DBT conversion rate only reached 87%. This desulfurization result is lower than the desulfurization rate that was obtained during the initial catalysis. However, when the reaction time was extended to 45 min, the desulfurization rates obtained in five ODS recovery experiments were 99.81%, 99.81%, 99.78%, 99.07% and 98.87%, respectively (Figure 12). This is not significantly different from the initial desulfurization rate. Moreover, the IR of the catalyst before and after the recovery were similar, which indicated that the structure of the catalyst was not destroyed during the catalytic desulfurization reaction. Therefore, the $[\text{BMIM}]_2\text{SMo}_{12}\text{O}_{40}$ catalyst has excellent recovery activity.

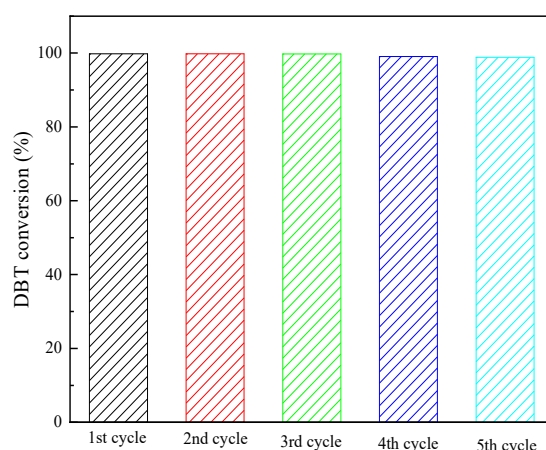


Figure 12. Desulfurization performance of the recycled [BMIM]₂SMo₁₂O₄₀ catalyst.

2.5. Oxidative Desulfurization of Real Diesel

The desulfurization performance of [TBA]₂SMo₁₂O₄₀ and [BMIM]₂SMo₁₂O₄₀ catalysts were evaluated in real diesel. Due to the complex and diverse components of real diesel, the removal effect of sulfur compounds is affected. The initial sulfur content of real diesel is 514.53 ppm. The reaction conditions are set as the amount of catalyst being 0.63 g (the amount of catalyst accounts for 1.5 wt% of the simulated oil quality), O/S = 15, and at room temperature. Using [TBA]₂SMo₁₂O₄₀ as a catalyst, the sulfur content of real diesel was reduced from 514.53 ppm to 93.17 ppm after 150 min of reaction (Table 2). In order to further remove the sulfur compounds, the oil after the reaction was collected for the second ODS treatment, and the sulfur content in the oil was reduced to 20.18 ppm after 15 min. The total desulfurization rate of the [TBA]₂SMo₁₂O₄₀ catalyst reached 96.08% after two ODS treatments. Under the catalysis of [BMIM]₂SMo₁₂O₄₀, the sulfur content in the oil was decreased from 514.53 ppm to 41.52 ppm by two ODS treatments, maintaining the same reaction conditions (the reaction time of the first and second ODS process is 150 min and 60 min, respectively) (Table 2). The total desulfurization rate of the [BMIM]₂SMo₁₂O₄₀ catalyst reached 91.93% after two ODS treatments. Hence, [TBA]₂SMo₁₂O₄₀ and [BMIM]₂SMo₁₂O₄₀ have favorable application prospects as catalysts.

Table 2. Desulfurization performance of catalysts in actual diesel.

Catalyst	Initial Sulfur Content	By ODS	By ODS Twice	Total Desulfurization Rate
[TBA] ₂ SMo ₁₂ O ₄₀	514.53	93.17	20.18	96.08%
[BMIM] ₂ SMo ₁₂ O ₄₀	514.53	115.2	41.52	91.93%

2.6. The Mechanism of Oxidative Desulfurization Using SMo₁₂O₄₀²⁻-Organic Hybrid Catalysts

Figure 13 shows the ODS process of DBT using SMo₁₂O₄₀²⁻-organic hybrid catalysts. In the ODS system, DBT in model oil was extracted into the acetonitrile phase. The cation of the amphiphilic hybrid catalyst is lipophilic, which can capture the DBT close to the oxidation active center, thereby increasing the contact area between the oxidant and sulfur compound and improving the desulfurization rate. When the SMo₁₂O₄₀²⁻ reacts with the oxidant H₂O₂, it will generate the peroxy-active species with a stronger oxidizing ability. This peroxy-active species is the real oxidant in the ODS reaction. DBT can be oxidized to DBT sulfone by the action of the oxidant. The oxidation product sulfone is dissolved in the acetonitrile phase to achieve separation from the oil.

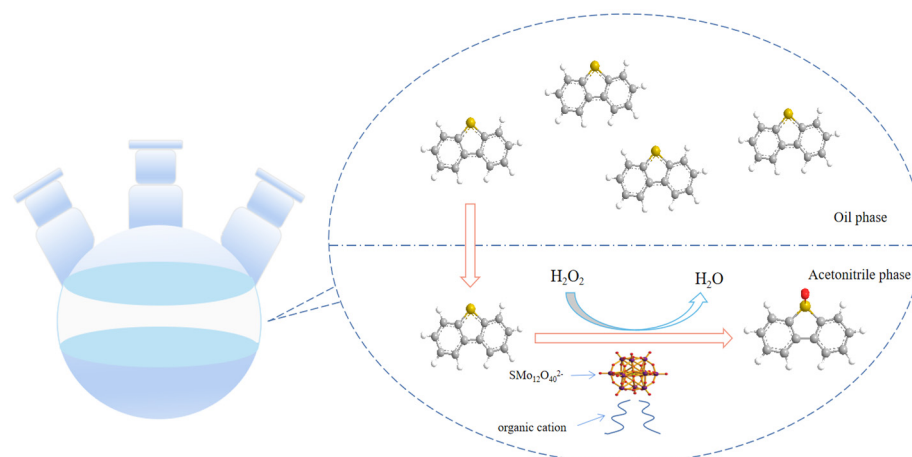


Figure 13. The ODS process of DBT using $\text{SMO}_{12}\text{O}_{40}^{2-}$ -organic hybrid catalysts.

3. Experimental

3.1. Synthesis of Catalysts

$[\text{TBA}]_2\text{SMO}_{12}\text{O}_{40}$ was prepared by the method described in the literature [44]. A certain amount of $\text{Na}_2\text{MoO}_4 \cdot 2\text{H}_2\text{O}$ (6.05 g, 25 mmol) was dissolved in 200 mL distilled water and stirred for 5 min at room temperature. NH_4VO_3 (0.6 g, 5.1 mmol) dissolved in H_2SO_4 (50 mL, 2 mol/L) was added and stirred for 5 min. Next, CH_3COCH_3 (250 mL) was added to the aforementioned system. After the mixture was stirred for 60 min at room temperature, tetrabutylammonium bromide (abbreviated as TBAB, 10 g, 31 mmol) was added. In order to complete metathesis, the above mixture was stirred continuously for 30 min. The precipitation was filtered and washed by distilled water and ethanol. The obtained solid catalyst was dried in a vacuum oven. The synthesis method of $[\text{BMIM}]_2\text{SMO}_{12}\text{O}_{40}$ (6.8 g, 31 mmol) and $[\text{ODA}]_2\text{SMO}_{12}\text{O}_{40}$ (12.2 g, 31 mmol) is similar to the above method, and only requires the replacement of the addition of TBAB with 1-butyl-3-methylimidazolium bromide (BMIMBr) or octadecyl trimethyl ammonium bromide (ODAB) in the reaction system.

3.2. Characterization

Infrared absorption spectra (IR) were performed for the $400\text{--}4000\text{ cm}^{-1}$ region on a Nicolet iS10 spectrometer (Thermo Fisher Scientific Co., Ltd., Waltham, MA, USA) with a resolution of 4 cm^{-1} and 32 scans. X-ray diffraction (XRD) patterns were recorded on a Brooke D8 advance power diffractometer (Bruker AXS Co., Ltd, Karlsruhe, Germany) in the range of 2θ from 5° to 60° . The SEM images were acquired by a 450 FEG electron microscope (United States FEI Co., Ltd., Hillsboro, OR, USA). Thermogravimetric analysis was carried out using a TG 209F3 thermal analyzer (Germany NETZSCH Co., Ltd., Selb, Germany) in the temperature range between $30\text{ }^\circ\text{C}$ and $600\text{ }^\circ\text{C}$ with a heating rate of $10\text{ }^\circ\text{C min}^{-1}$ under nitrogen. X ray photoelectron spectrometric (XPS) were analyzed by a Thermo Fischer Escalab 250Xi spectrometer (Thermo Fisher Scientific Co., Ltd.).

3.3. Oxidative Desulfurization Process for Model Oil

The model oil is prepared by dissolving a certain amount of DBT (BT or 4,6-DMDBT) in 60 mL of n-octane. The initial sulfur content of the model oil is 500 ppm. The ODS system employs H_2O_2 as the oxidant and acetonitrile as the extractant. In a typical ODS experiment, 60 mL model oil with a sulfur content of 500 ppm, 60 mL acetonitrile, a certain dosage of catalyst, and H_2O_2 were added into a 250 mL three-neck flask. The three-neck flask was placed in a water bath with magnetic stirring. In order to reduce the evaporation of oil at different temperatures, the middle port of the three-neck flask was connected with a condenser tube and the left and right ports are plugged with plugs. Samples were taken from the upper oil phase at a certain time. The sulfur content of the sample was analyzed in

a WK-2E microcoulometer. The conversion rate of DBT (BT or 4,6-DMDBT) was calculated using the following formula.

$$\text{Conversion (\%)} = (C_0 - C_t) / C_0 \times 100\%$$

where C_0 is the initial sulfur content in oil, and C_t is the sulfur content at the different samples.

4. Conclusions

This paper presented an effective method for the deep desulfurization of model oil using the amphiphatic $\text{SMo}_{12}\text{O}_{40}^{2-}$ -organic hybrid catalysts at room temperature. The prepared catalysts had a favorable desulfurization performance for sulfur compounds. Under optimized reaction conditions, when using $[\text{TBA}]_2\text{SMo}_{12}\text{O}_{40}$ as a catalyst, the DBT conversion rate reached 99.89% in only 10 min, and when $[\text{BMIM}]_2\text{SMo}_{12}\text{O}_{40}$ was employed as a catalyst, the DBT can achieve 99.81% removal within 15 min. The $[\text{ODA}]_2\text{SMo}_{12}\text{O}_{40}$ catalyst can make the DBT conversion rate reach 99.47% within 60 min. The catalysts also have an excellent removal effect on BT and 4,6-DMDBT. The oxidation activity of the sulfur compound is affected by the electron density and steric hindrance. The desulfurization results of catalysts show that DBT is more easily oxidized than BT and 4,6-DMDBT. Under the condition of $[\text{ODA}]_2\text{SMo}_{12}\text{O}_{40}$ as a catalyst, 4,6-DMDBT is easier to remove than BT, which is different from the desulfurization performance of the other two catalysts. The reason is that it is easier for the long alkyl chain to wrap up the larger molecule of 4,6-DMDBT close to the active center. The recycle performance of catalysts were investigated. The $[\text{TBA}]_2\text{SMo}_{12}\text{O}_{40}$ immobilized in the acetonitrile phase was still reactive after the reaction, and can be reused at least five times for ODS. $[\text{BMIM}]_2\text{SMo}_{12}\text{O}_{40}$ behaves as a heterogeneous catalyst in the ODS process, and can be recovered by simple filtration. $[\text{BMIM}]_2\text{SMo}_{12}\text{O}_{40}$ still maintains excellent activity after five ODS cycles. When $[\text{TBA}]_2\text{SMo}_{12}\text{O}_{40}$ and $[\text{BMIM}]_2\text{SMo}_{12}\text{O}_{40}$ are applied to real diesel, they can achieve 99% and 98% desulfurization rates by ODS twice, respectively, indicating that the $[\text{SMo}_{12}\text{O}_{40}]^{2-}$ -organic hybrid catalysts have a favorable application prospect in industry. The ODS system using an $\text{SMo}_{12}\text{O}_{40}^{2-}$ -based catalyst provides a simple, mild and fast approach for deep desulfurization. However, the preparation cost of an $\text{SMo}_{12}\text{O}_{40}^{2-}$ -based catalyst is comparatively approximately 20% higher compared to that of the current commercial catalyst, and further R&D is needed for an $\text{SMo}_{12}\text{O}_{40}^{2-}$ -based catalyst with regard to laboratory and industrial applications.

Author Contributions: Investigation, writing—original draft preparation, J.Z.; writing—review and editing, B.W., I.V.K. and K.V.; supervision, project administration, funding acquisition, R.W. All authors have read and agreed to the published version of the manuscript.

Funding: This research was funded by National Natural Science Foundation of China (Nos. 20976097; 21076116 and 21211120165; 21311120297), the Natural Science Foundation of Shandong Province (ZR2018MEE048), and the PetroChina Innovation Foundation (2010D-5006-0405).

Institutional Review Board Statement: Not applicable.

Informed Consent Statement: Not applicable.

Data Availability Statement: Not applicable.

Conflicts of Interest: The authors declare that they have no conflict of interest.

References

1. Li, J.; Yang, Z.; Li, S.; Jin, Q.; Zhao, J. Review on oxidative desulfurization of fuel by supported heteropolyacid catalysts. *J. Ind. Eng. Chem.* **2020**, *82*, 1–16. [[CrossRef](#)]
2. Xu, Y.; Ma, W.-W.; Dolo, A.; Zhang, H. An amphiphilic catalyst based on sandwich-type polyoxometalate for deep desulfurization of fuels in ionic liquid. *RSC Adv.* **2016**, *6*, 71–76. [[CrossRef](#)]

3. Yashnik, S.A.; Kerzhentsev, M.A.; Salnikov, A.V.; Ismagilov, Z.R.; Bourane, A.; Koseoglu, O.R. Cu-Zn-Al-O Catalysts for the Oxidative Desulfurization of Dibenzothiophene, a Typical Sulfur-Containing Compound of the Diesel Fraction. *Kinet. Catal.* **2015**, *56*, 4–75. [[CrossRef](#)]
4. Zhang, J.; Wang, A.; Wang, Y.; Wang, H.; Gui, J. Heterogeneous oxidative desulfurization of diesel oil by hydrogen peroxide: Catalysis of an amphiphatic hybrid material supported on SiO₂. *Chem. Eng. J.* **2014**, *245*, 65–70. [[CrossRef](#)]
5. Yang, R.T.; Hernandez-Maldonado, A.J.; Yang, F.H. Desulfurization of transportation fuels with zeolites under ambient conditions. *Science* **2003**, *301*, 5629–5681. [[CrossRef](#)]
6. Song, C.; Ma, X.L. New design approaches to ultra-clean diesel fuels by deep desulfurization and deep dearomatization. *Appl. Catal. B-Environ.* **2003**, *41*, 1–2–38. [[CrossRef](#)]
7. Liu, A.; Zhang, Z.; Fang, Z.; Liu, B.; Huang, K. Synthesis of 5-ethoxymethylfurfural from 5-hydroxymethylfurfural and fructose in ethanol catalyzed by MCM-41 supported phosphotungstic acid. *J. Ind. Eng. Chem.* **2014**, *20*, 4–84. [[CrossRef](#)]
8. Jin, T.; Yang, Q.; Meng, C.; Xu, J.; Liu, H.; Hu, J.; Ling, H. Promoting desulfurization capacity and separation efficiency simultaneously by the novel magnetic Fe₃O₄@PAA@MOF-199. *RSC Adv.* **2014**, *4*, 41902–41909. [[CrossRef](#)]
9. Yang, H.; Jiang, B.; Sun, Y.; Zhang, L.; Sun, Z.; Wang, J.; Tantai, X. Polymeric cation and isopolyanion ionic self-assembly: Novel thin-layer mesoporous catalyst for oxidative desulfurization. *Chem. Eng. J.* **2017**, *317*, 32–41. [[CrossRef](#)]
10. Zhao, R.; Wang, J.; Zhang, D.; Sun, Y.; Han, B.; Tang, N.; Zhao, J.; Li, K. Deep Catalytic Oxidative Desulfurization of Model Fuel Based on Modified Iron Porphyrins in Ionic Liquids: Anionic Ligand Effect. *ACS Sustain. Chem. Eng.* **2017**, *5*, 3–5. [[CrossRef](#)]
11. Bej, S.K. Revamping of diesel hydrodesulfurizers: Options available and future research needs. *Fuel Process. Technol.* **2004**, *85*, 13–17. [[CrossRef](#)]
12. Francisco, M.; Arce, A.; Soto, A. Ionic liquids on desulfurization of fuel oils. *Fluid Phase Equilibria* **2010**, *294*, 1–2–48. [[CrossRef](#)]
13. Mondal, S.; Hangan-Balkir, Y.; Alexandrova, L.; Link, D.; Howard, B.; Zandhuis, P.; Cugini, A.; Horwitz, C.P.; Collins, T.J. Oxidation of sulfur components in diesel fuel using Fe-TAML (R) catalysts and hydrogen peroxide. *Catal. Today* **2006**, *116*, 4–61. [[CrossRef](#)]
14. Gao, S.; Chen, X.; Xi, X.; Abro, M.; Afzal, W.; Abro, R.; Yu, G. Coupled Oxidation-Extraction Desulfurization: A Novel Evaluation for Diesel Fuel. *ACS Sustain. Chem. Eng.* **2019**, *7*, 6–8. [[CrossRef](#)]
15. Li, L.; Lu, Y.; Meng, H.; Li, C. Lipophilicity of amphiphilic phosphotungstates matters in catalytic oxidative desulfurization of oil by H₂O₂. *Fuel* **2019**, *253*, 802–810. [[CrossRef](#)]
16. Rajendran, A.; Cui, T.-Y.; Fan, H.-X.; Yang, Z.-F.; Feng, J.; Li, W.-Y. A comprehensive review on oxidative desulfurization catalysts targeting clean energy and environment. *J. Mater. Chem. A* **2020**, *8*, 2246–2285. [[CrossRef](#)]
17. Mjalli, F.S.; Ahmed, O.U.; Al-Wahaibi, T.; Al-Wahaibi, Y.; AlNashef, I.M. Deep oxidative desulfurization of liquid fuels. *Rev. Chem. Eng.* **2014**, *30*, 4–78. [[CrossRef](#)]
18. Ma, X.L.; Velu, S.; Kim, J.H.; Song, C.S. Deep desulfurization of gasoline by selective adsorption over solid adsorbents and impact of analytical methods on ppm-level sulfur quantification for fuel cell applications. *Appl. Catal. B-Environ.* **2005**, *56*, 134–147. [[CrossRef](#)]
19. Hossain, M.N.; Park, H.C.; Choi, H.S. A Comprehensive Review on Catalytic Oxidative Desulfurization of Liquid Fuel Oil. *Catalysts* **2019**, *9*, 229. [[CrossRef](#)]
20. Dehkordi, A.M.; Kiaei, Z.; Sobati, M.A. Oxidative desulfurization of simulated light fuel oil and untreated kerosene. *Fuel Process. Technol.* **2009**, *90*, 3–45. [[CrossRef](#)]
21. Craven, M.; Xiao, D.; Kunstmann-Olsen, C.; Kozhevnikova, E.F.; Blanc, F.; Steiner, A.; Kozhevnikov, I.V. Oxidative desulfurization of diesel fuel catalyzed by polyoxometalate immobilized on phosphazene-functionalized silica. *Appl. Catal. B-Environ.* **2018**, *231*, 82–91. [[CrossRef](#)]
22. Campos-Martin, J.M.; Capel-Sanchez, M.C.; Perez-Presas, P.; Fierro, J.L.G. Oxidative processes of desulfurization of liquid fuels. *J. Chem. Technol. Biotechnol.* **2010**, *85*, 7–90. [[CrossRef](#)]
23. Jiang, X.; Li, H.; Zhu, W.; He, L.; Shu, H.; Lu, J. Deep desulfurization of fuels catalyzed by surfactant-type decatungstates using H₂O₂ as oxidant. *Fuel* **2009**, *88*, 3–6. [[CrossRef](#)]
24. Lei, P.X.; Chen, C.C.; Yang, J.; Ma, W.H.; Zhao, J.C.; Zang, L. Degradation of dye pollutants by immobilized polyoxometalate with H₂O₂ under visible-light irradiation. *Environ. Sci. Technol.* **2005**, *39*, 21–74. [[CrossRef](#)]
25. Chen, Y.; Song, H.; Meng, H.; Lu, Y.; Li, C.; Lei, Z.; Chen, B. Polyethylene glycol oligomers as green and efficient extractant for extractive catalytic oxidative desulfurization of diesel. *Fuel Process. Technol.* **2017**, *158*, 20–25. [[CrossRef](#)]
26. Kozhevnikov, I.V. Catalysis by heteropoly acids and multicomponent polyoxometalates in liquid-phase reactions. *Chem. Rev.* **1998**, *98*, 1–98. [[CrossRef](#)]
27. Tang, N.; Jiang, Z.; Li, C. Oxidation of refractory sulfur-containing compounds with molecular oxygen catalyzed by vanadoperiodate. *Green Chem.* **2015**, *17*, 2–20. [[CrossRef](#)]
28. Izarova, N.V.; Pope, M.T.; Kortz, U. Noble Metals in Polyoxometalates. *Angew. Chem.-Int. Ed.* **2012**, *51*, 38–510. [[CrossRef](#)]
29. Himeno, S.; Takamoto, M.; Santo, R.; Ichimura, A. Redox Properties and Basicity of Keggin-Type Polyoxometalate Complexes. *Bull. Chem. Soc. Jpn.* **2005**, *78*, 1–100. [[CrossRef](#)]
30. Ruther, T.; Hultgren, V.M.; Timko, B.P.; Bond, A.M.; Jackson, W.R.; Wedd, A.G. Electrochemical investigation of photooxidation processes promoted by sulfo-polyoxometalates: Coupling of photochemical and electrochemical processes into an effective catalytic cycle. *J. Am. Chem. Soc.* **2003**, *125*, 33–43. [[CrossRef](#)]

31. Zhang, J.; Bond, A.M.; MacFarlane, D.R.; Forsyth, S.A.; Pringle, J.M.; Mariotti, A.W.A.; Glowinski, A.F.; Wedd, A.G. Voltammetric studies on the reduction of polyoxometalate anions in ionic liquids. *Inorg. Chem.* **2005**, *44*, 14–32. [[CrossRef](#)] [[PubMed](#)]
32. Wei, S.; He, H.; Cheng, Y.; Yang, C.; Zeng, G.; Qiu, L. Performances, kinetics and mechanisms of catalytic oxidative desulfurization from oils. *RSC Adv.* **2016**, *6*, 105–169. [[CrossRef](#)]
33. Afsharpour, M.; Amraee, A.R. Synthesis of bio-inspired N-doped SiC and investigation of its synergetic effects on Mo catalysts in oxidative desulfurization reaction. *Mol. Catal.* **2017**, *436*, 285–293. [[CrossRef](#)]
34. Ding, Y.; Zhu, W.; Li, H.; Jiang, W.; Zhang, M.; Duan, Y.; Chang, Y. Catalytic oxidative desulfurization with a hexatungstate/aqueous H₂O₂/ionic liquid emulsion system. *Green Chem.* **2011**, *13*, 5–6. [[CrossRef](#)]
35. Gao, H.; Guo, C.; Xing, J.; Zhao, J.; Liu, H. Extraction and oxidative desulfurization of diesel fuel catalyzed by a Bronsted acidic ionic liquid at room temperature. *Green Chem.* **2010**, *12*, 1220–1224. [[CrossRef](#)]
36. Zhang, Y.; Lue, H.; Wang, L.; Zhang, Y.; Liu, P.; Han, H.; Jiang, Z.; Li, C. The oxidation of benzothiophene using the Keggin-type lacunary polytungstophosphate as catalysts in emulsion. *J. Mol. Catal. A—Chem.* **2010**, *332*, 1–2–64. [[CrossRef](#)]
37. Nisar, A.; Zhuang, J.; Wang, X. Construction of Amphiphilic Polyoxometalate Mesostructures as a Highly Efficient Desulfurization Catalyst. *Adv. Mater.* **2011**, *23*, 1130–1135. [[CrossRef](#)]
38. Zhou, Y.; Guo, Z.; Hou, W.; Wang, Q.; Wang, J. Polyoxometalate-based phase transfer catalysis for liquid-solid organic reactions: A review. *Catal. Sci. Technol.* **2015**, *5*, 9–35. [[CrossRef](#)]
39. Li, C.; Jiang, Z.X.; Gao, J.B.; Yang, Y.X.; Wang, S.J.; Tian, F.P.; Sun, F.; Sun, X.; Ying, P.; Han, C. Ultra-deep desulfurization of diesel: Oxidation with a recoverable catalyst assembled in emulsion. *Chemistry* **2004**, *10*, 9–80. [[CrossRef](#)]
40. Lu, H.Y.; Gao, J.B.; Jiang, Z.X.; Jing, F.; Yang, Y.X.; Wang, G.; Li, C. Ultra-deep desulfurization of diesel by selective oxidation with C₁₈H₃₇N(CH₃)₃ (4) H₂NaPW₁₀O₃₆ catalyst assembled in emulsion droplets. *J. Catal.* **2006**, *239*, 2–75. [[CrossRef](#)]
41. Qiu, J.; Wang, G.; Zeng, D.; Tang, Y.; Wang, M.; Li, Y. Oxidative desulfurization of diesel fuel using amphiphilic quaternary ammonium phosphomolybdate catalysts. *Fuel Process. Technol.* **2009**, *90*, 12–42. [[CrossRef](#)]
42. Ribeiro, S.O.; Juliao, D.; Cunha-Silva, L.; Domingues, V.F.; Valenca, R.; Ribeiro, J.C.; de Castro, B.; Balula, S.S. Catalytic oxidative/extractive desulfurization of model and untreated diesel using hybrid based zinc-substituted polyoxometalates. *Fuel* **2016**, *166*, 268–275. [[CrossRef](#)]
43. Zhu, W.; Huang, W.; Li, H.; Zhang, M.; Jiang, W.; Chen, G.; Han, C. Polyoxometalate-based ionic liquids as catalysts for deep desulfurization of fuels. *Fuel Process. Technol.* **2011**, *92*, 10–18. [[CrossRef](#)]
44. Yang, S.; Hao, Y.; Wang, J.; Wang, H.; Zheng, Y.; Tian, H.; Liu, Y.; Sun, B. Selective catalytic dehydration of furfuryl alcohol to 2,2'-difurfuryl ether using a polyoxometalate catalyst. *Sci. Rep.* **2017**, *7*, 12954. [[CrossRef](#)]
45. Mirante, F.; Dias, L.; Silva, M.; Ribeiro, S.O.; Corvo, M.C.; de Castro, B.; Granadeiro, C.M.; Balula, S.S. Efficient heterogeneous polyoxometalate-hybrid catalysts for the oxidative desulfurization of fuels. *Catal. Commun.* **2018**, *104*, 1–8. [[CrossRef](#)]
46. Lu, H.; Deng, C.; Ren, W.; Yang, X. Oxidative desulfurization of model diesel using (C₄H₉)₄N (6)Mo₇O₂₄ as a catalyst in ionic liquids. *Fuel Process. Technol.* **2014**, *119*, 87–91. [[CrossRef](#)]
47. Li, D.-P.; Hu, X.-L.; Zhao, Y.-M.; Guan, P.; Yu, J.-Y. Study of Green Solvents 1-butyl-3-methylimidazolium Ionic Liquids' Structure and Properties. In Proceedings of the 2010 4th International Conference on Bioinformatics and Biomedical Engineering, Chengdu, China, 18–20 June 2010.
48. Cao, J.-X.; Liu, C.-L.; Liao, L.-L. Preparation, characterization and photocatalytic activity of Keggin type of phosphotungstic acid salts. *J. Jilin Univ.* **2013**, *51*, 5–8.
49. Lu, H.; Ren, W.; Wang, H.; Wang, Y.; Chen, W.; Suo, Z. Deep desulfurization of diesel by ionic liquid extraction coupled with catalytic oxidation using an Anderson-type catalyst (C₄H₉)₄N (4)NiMo₆O₂₄H₆. *Appl. Catal. A—Gen.* **2013**, *453*, 376–382. [[CrossRef](#)]
50. Qiu, L.; Zou, K.; Xu, G. Investigation on the sulfur state and phase transformation of spent and regenerated S zorb sorbents using XPS and XRD. *Appl. Surf. Sci.* **2013**, *266*, 230–234. [[CrossRef](#)]
51. González-Ildelfonso, M.; Escobar, J.; Gordillo-Cruz, E.; del Ángel, P.; Suárez-Toriello, V.A.; De los Reyes, J.A. RuS₂-modified NiW/Al₂O₃ catalysts for refractory 4,6-dimethyl-dibenzothiophene hydrodesulfurization. *Mater. Chem. Phys.* **2022**, *278*, 125568. [[CrossRef](#)]
52. Abazari, R.; Esrafil, L.; Morsali, A.; Wu, Y.; Gao, J. PMO₁₂@UiO-67 nanocomposite as a novel non-leaching catalyst with enhanced performance durability for sulfur removal from liquid fuels with exceptionally diluted oxidant. *Appl. Catal. B Environ.* **2021**, *283*, 119582. [[CrossRef](#)]
53. Peng, Y.-L.; Liu, J.; Zhang, H.-F.; Luo, D.; Li, D.J.I.C.F. A size-matched POM@ MOF composite catalyst for highly efficient and recyclable ultra-deep oxidative fuel desulfurization. *Inorg. Chem. Front.* **2018**, *5*, 7–9. [[CrossRef](#)]
54. Zhang, J.-A.; Pan, M.; Jiang, J.-J.; She, Z.-G.; Fan, Z.-J.; Su, C.-Y. Syntheses, crystal structures and antimicrobial activities of thioether ligands containing quinoline and pyridine terminal groups and their transition metal complexes. *Inorg. Chim. Acta* **2011**, *374*, 1–77. [[CrossRef](#)]
55. Xun, S.; Jiang, W.; Guo, T.; He, M.; Ma, R.; Zhang, M.; Zhu, W.; Li, H. Magnetic mesoporous nanospheres supported phosphomolybdate-based ionic liquid for aerobic oxidative desulfurization of fuel. *J. Colloid Interface Sci.* **2019**, *534*, 239–247. [[CrossRef](#)] [[PubMed](#)]
56. Yue, S.; Song, Q.; Zang, S.; Deng, G.; Li, J. Synthesis of polyoxomolybdate-quinoline compounds beads for catalytic oxidative desulfurization. *Mol. Catal.* **2018**, *455*, 88–94. [[CrossRef](#)]

57. Zhuang, J.; Hu, B.; Tan, J.; Jin, X. Deep oxidative desulfurization of dibenzothiophene with molybdovanadophosphoric heteropolyacid-based catalysts. *Transit. Met. Chem.* **2014**, *39*, 2–20. [[CrossRef](#)]
58. Xu, D.; Zhu, W.; Li, H.; Zhang, J.; Zou, F.; Shi, H.; Yan, Y. Oxidative Desulfurization of Fuels Catalyzed by V_2O_5 in Ionic Liquids at Room Temperature. *Energy Fuels* **2009**, *23*, 12–33. [[CrossRef](#)]
59. Otsuki, S.; Nonaka, T.; Takashima, N.; Qian, W.H.; Ishihara, A.; Imai, T.; Kabe, T. Oxidative desulfurization of light gas oil and vacuum gas oil by oxidation and solvent extraction. *Energy Fuels* **2000**, *14*, 6–9. [[CrossRef](#)]

Disclaimer/Publisher’s Note: The statements, opinions and data contained in all publications are solely those of the individual author(s) and contributor(s) and not of MDPI and/or the editor(s). MDPI and/or the editor(s) disclaim responsibility for any injury to people or property resulting from any ideas, methods, instructions or products referred to in the content.